Published in final edited form as:
J Control Release. 2005 September 20; 107(1): 143–157.

Polyplex Nanogel formulations for drug delivery of cytotoxic nucleoside analogs

Serguei V. Vinogradov*, **Arin D. Zeman**, **Elena V. Batrakova**, and **Alexander V. Kabanov**
Center for Drug Delivery and Nanomedicine and College of Pharmacy, Department of Pharmaceutical Sciences, 985830 Nebraska Medical Center, Omaha, NE 68198-5830;

Abstract

Hydrophilic nanosized particles consisting of the cross-linked cationic polymer network (Nanogels) are suggested as a drug delivery system for nucleoside analog 5'-triphosphates, an active form of cytotoxic anticancer drugs. Preparation, properties, and cellular effects of several polyplex Nanogel formulations with the 5'-triphosphate of cytotoxic 5-fluoroadenosine arabinoside (fludarabine) (FATP) were examined and discussed here. The polyplexes have formed spontaneously by mixing solutions of FATP and Nanogels because of ionic interactions between protonated polyethylenimine (PEI) chains in Nanogel network with polyphosphate groups of the drug. Subsequent compaction of the flexible Nanogel network has resulted in an encapsulation of the FATP/PEI complex in a dense core surrounded by hydrophilic polymer (PEG) envelope. This structure has provided a sustained release of the drug, as well as an efficient protection of FATP against enzymatic degradation. The drug loading could reach up to 33% by weight of the drug-Nanogel formulation. *In vitro* 35% of loaded drug has released from Nanogel formulations during the first 24 hours, and a slower additional release was observed during the next two days. Nanogels have protected 90% of the encapsulated FATP from enzymatic dephosphorylation during the first 60 min of incubation *in vitro*. The drug-Nanogel formulation compared to the drug has demonstrated a significantly enhanced cytotoxicity in cultured cancer cells. Cancer cell-targeting molecules, such as folate, could be easily attached to Nanogels and this modification has resulted in a strong 10-fold increase of the carrier's internalization in human breast carcinoma MCF-7 cells. Moreover, transcellular transport of the folate-Nanogel polyplexes was found to be 4 times more effective compared to the drug alone using Caco-2 cell monolayers as an i*n vitro* intestinal model. The data demonstrate that this carrier-based approach to delivery of cytotoxic drugs may enhance tumor specificity and significantly reduce side effects related to systemic toxicity usually observed during cancer chemotherapy.

Keywords

Nanogel; Nucleoside 5'-triphosphate; Fludarabine; Folate vector; Cytotoxicity; MCF-7; Caco-2

Introduction

Hydrophilic ionizable polymeric carriers that are able to bind biomolecules of opposite charge, forming polyionic complexes or polyplexes, and deliver them into various biological environments are receiving an increased attention as therapeutic drug delivery systems [1,2]. In particular, polymeric carriers on the basis of polyethylenimine (PEI) have demonstrated strong potential for therapeutic gene delivery and transfection [3–5]. However, these polycationic drug carriers are far from ideal, and further developments need to reduce their toxicity, optimize circulation parameters and polyplex size [6–8].

*Corresponding author. Phone: 1-402-559-9362; fax: 1-402-559-9365; *E-mail address*:vinograd@unmc.edu.

Lately, a nanosized carrier based on a crosslinked network of branched PEI and poly(ethylene glycol) (PEG) molecules was synthesized and characterized [9,10]. This polymeric network has been called Nanogel and demonstrated an excellent swelling capacity and low buoyant density in aqueous media that made it a promising system for systemic drug delivery. For example, antisense oligonucleotide has been bound to Nanogel cooperatively with phosphate groups bonded to PEI's protonated amino groups. Because of polymer chain flexibility, the Nanogel network has markedly collapsed as a result of oligonucleotide binding, so that the volume of polyplex decreased by an order of magnitude comparing to the volume of initial Nanogel. This volume has also depended on the oligonucleotide loading and environmental factors such as pH and salt concentration. The hydrophilic polymer envelope prevents the interaction between the drug-containing core and the blood components and allows for steric stabilization. Alike, many negatively charged hydrophobic compounds were capable to form stable water-soluble complexes with Nanogel [11]. Physicochemical properties of Nanogel and biological activity of oligonucleotide-Nanogel formulations have been recently reviewed [12]. Obviously, more systematic studies are needed to fully understand drug delivery capabilities of Nanogel, as well as an application of this carrier to systemic cancer chemotherapy.

Cancer chemotherapy is heavily relied on application of cytotoxic antimetabolites such as nucleoside analogs [13,14]. Many therapeutic nucleoside analogs actually represent prodrugs that are activated by enzymatic phosphorylation to finally form nucleoside analog 5'-triphosphates [15]. The intracellular nucleoside analogs 5'-triphosphates can efficiently terminate intracellular synthesis of nucleic acids and switch on the apoptotic cascade in cancer cells [16]. However, the efficacy of nucleoside analogs in cancer therapy is limited by ineffective intracellular conversion of these molecules into 5'-triphosphates. Tissue selectivity of many nucleoside analogs is determined primarily by the activity of corresponding kinases, for example, the lymphoselectivity of fludarabine is explained by the uniquely high deoxycytidine kinase activity in cells of lymphoid origin [17]. The drugs are generally administered in non-phosphorylated or more soluble 5'-monophosphorylated therapeutic form, because nucleoside analog 5'-triphosphates are usually considered too unstable as a drug form to be used directly in cancer chemotherapy. As a result high doses of nucleoside analogs need to be used resulting in systemic toxicity and other adverse effects. Furthermore, the non-specific tissue biodistribution of cytotoxic drugs significantly increases their systemic toxicity. Additionally, the development of various mechanisms of drug resistance has been demonstrated for different nucleoside analogs [18,19]. The nucleoside analog-using chemotherapy could be enhanced through administration of nucleoside analogs encapsulated in drug delivery system, such as liposomes, to increase cellular accumulation and cancer-specific targeting of the drugs [20,21]. Advanced drug carriers should have the following major properties: (i) easy and efficient drug loading; (ii) nanoscale size to allow efficient transport into cells; (iii) efficient protection of encapsulated drug in biological media; (iv) possibility of vectorization of drug carriers for site-specific delivery; (v) an efficient intracellular release of active drug into targeted cells.

In this manuscript, formation of polyplexes between synthetic polymer carrier and nucleoside 5'-triphosphates is reported for the first time. The swollen Nanogel particles contain protonated amino groups that are dispersed all over the volume of cross-linked polymer network and easily accessible to form complexes with negatively charged polyanions (Figure 1). The aim of this study was to evaluate properties of Nanogels formulated with phosphorylated nucleoside analogs and application of these formulations to cancer chemotherapy. The potential use of the vectorized Nanogels for oral drug delivery was studies *in vitro* by measuring the transport of carriers loaded with a nucleoside analog 5'-triphosphate across Caco-2 monolayers since this model is the most commonly used to evaluate intestinal drug permeability [22].

2. Materials and methods

2.1. Materials

All solvents and reagents, except specially mentioned, were purchased from Sigma-Aldrich (St.Louis, MO) and used without purification.

2.2. Nanogel synthesis

Nanogel network was obtained using a modified "emulsification-solvent evaporation" method [23]. PEG (MW 8,000) was dried *in vacuo* over phosphorus oxide for 24 h, dissolved in anhydrous acetonitrile, and treated with 6-molar excess of 1,1'-carbonyldiimidazole for 2 h at 40°C. The activated polymers were precipitated in ice-cold anhydrous ether, collected by centrifugation, washed twice by ether, and finally dried *in vacuo*. Commercial high-molecular weight PEI (branched, MW 25,000) was dissolved in water and purified by dialysis in SpectraPor membrane tube with a MW cutoff of 3,500. 40% (w/v) solution of the activated polymer in 4 ml of dichloromethane was dispersed at vigorous mixing in aqueous solution of PEI (50 ml), and sonicated in Bransonic ultrasonic bath for 5 min. PEI concentration has been adjusted to obtain PEG to PEI weight ratio from 2 to 12. Organic solvent was immediately removed *in vacuo* using Buchi Rotavapor at 40°C, and transparent solution was left stirring overnight. The debris was removed by centrifugation at 3,000 rpm for 30 min. The polymer product was dialyzed overnight in a SpectraPor membrane tube with a MW cutoff of 50,000 against aqueous 0.01% ammonia. The obtained Nanogel product was concentrated *in vacuo*, redissolved in methanol and precipitated in cold ether. The dried *in vacuo* product was characterized by proton NMR and elemental analysis without additional purification.

For analysis of PEG/PEI ratio in Nanogel preparations, 5% solutions of dried samples in D_2O were prepared and filtered. ^1H NMR spectra (with integration) were measured in the range 0–6 ppm at ambient temperature using the Varian 300 MHz spectrometer. Elemental analysis (M-H-W Laboratories, Phoenix, AZ) was used to determine the total nitrogen content in Nanogels.

2.3. Preparation of the folate-modified Nanogel

Solutions of 60 mg of Nanogel (400 μmol of total nitrogen) in 1 ml of PBS, pH 7.4, were mixed with 0.1 ml or 0.5 ml of 40 mM folic acid in the same buffer, and then treated respectively by 3 mg (16 μmol) or 15 mg (80 μmol) of water-soluble 1-(3-dimethylaminopropyl)-3-ethylcarbodiimide hydrochloride (EDC) overnight at 25°C. The reaction mixtures have been dialyzed in SpectraPor membrane tube with a MW cutoff of 3,500 against diluted aqueous ammonia (0.01%) with two buffer changes for 24 h. The purified Nanogel samples were freeze-dried and analyzed by UV absorbance at 363 nm (ε = 6,200) in PBS to measure the folate content [24]. Two samples of Nanogel have been obtained with folate modification of 1 and 5% of total amino groups. Rhodamine label was introduced into Nanogels using reaction with rhodamine isothiocyanate according to the previously described protocol [25].

2.4. Complexes of Nanogel with cupper (II) nitrate

A calibration curve was prepared using serial dilutions of PEI (titrated by HCl to pH 7.4) from 1 to 500 μg/ml in 0.1M NaCl, 10 mM tris-HCl, pH 7.4. 1 ml of these solutions was mixed with 3 ml of 20 μM $Cu(NO_3)_2$ in the same buffer. Absorbance of the forming blue solutions was measured at 285 nm using Perkin-Elmer spectrophotometer. The obtained values were corrected by subtracting the absorbance of a blank mixture without PEI. Absorbance (Y) was related to PEI concentration (X) by the equation: $Y = 0.0033X + 0.0256$. Linear range of Nanogel concentration from 100 to 500 μg/ml was used to analyze PEI content [26].

2.5. Swelling of PEG-g-PEI gels

A set of hydrogels with PEG/PEI weight ratio from 2 to 10 have been prepared. Totally 0.3 g of bis-activated PEG (MW 8,000) and PEI (MW 25,000) in 1 ml-volume of 30% aqueous solution has been reacted overnight at 25°C. The formed transparent gel was cut into three pieces, weighed, placed in water, PBS or 1% solution of acetic acid, and incubated for 48 h at 25°C. The swelling degree (*S*) was calculated by dividing the weight of swollen gel (*m*) by initial weight of polymer components taken in the reaction, using the equation $S = m/0.3 \times 100$, and plotted as a function of PEG/PEI weight ratio.

2.6. Synthesis of 2-fluoroadenine arabinoside 5'-triphosphate (FATP)

Fludarabine 5'-phosphate (FAMP, Fludara®, Berlex Laboratories) was used as initial compound in the synthesis of corresponding nucleoside analog 5'-triphosphate [27]. Sodium salt of FAMP (100 mg, 0.24 mmol) was dissolved in water and converted to tri-n-butylammonium salt by passing through a small column with Dowex 50x8 (tri-n-butylammonium salt). The product was concentrated *in vacuo*, dried by repetitive coevaporation with anhydrous acetonitrile and dissolved in 5 ml of dry dimethylformamide. 1,1'-Carbonyldiimidazole (120 mg, 0.72 mmol) dissolved in 5 ml of anhydrous acetonitrile was then added to the solution of nucleotide and the reaction mixture was allowed to stand for 2 h at 25°C. Sodium pyrophosphate (1.2 mmol) was converted to tri-n-butylammonium salt as described above, concentrated *in vacuo*, and dissolved in 10 ml of dry methanol to obtain 5% solution. Activated nucleotide solution was quenched with 0.1 ml of methanol for 10 min and treated with the methanolic solution of pyrophosphate. The reaction mixture was stirred for 24 h at 25°C. Organic solvents were removed *in vacuo*, the reaction mixture was dissolved in 0.05M triethylammonium bicarbonate (TEAB) buffer, pH 8, and fractionated using anion-exchange chromatography on the column (2.5x25 cm) with Toyopearl DEAE-650M equilibrated in 0.05M TEAB buffer. The product (FATP) was separated from mono-, di-and polyphosphate by-products using a gradient elution from 0.2 to 0.3M TEAB over 6-h period at elution rate 1.5 ml/min. Fractions containing FATP were collected, frozen, and lyophilized, providing the FATP with a yield of 74% and at >90% nucleoside purity.

2.7. HPLC analysis of nucleoside 5'-phosphates

The HPLC analysis of the nucleoside and corresponding 5'-mono-, di-, and triphosphates was performed in the ion-pair mode on Vydac C18 column (5 μm, 0.4 x 15 cm) using elution rate 1 ml/min and gradient elution (0 to 100% of buffer B over 20-min period) with the following buffers: (A) 40 mM KH_2PO_4, 0.2% tetrabutylammonium hydroxide, pH 7, and (B) 30% acetonitrile, 40 mM KH_2PO_4, 0.2% tetrabutylammonium hydroxide, pH 7, at 25°C [28]. Injection volume was 20 μl. Elution time for fludarabine was 4.8 min, fludarabine 5'-monophosphate −7 min, fludarabine 5'-diphosphate − 10.1 min, and fludarabine 5'-triphosphate − 13.2 min at these conditions.

2.8. Enzymatic hydrolysis of FATP

0.1, 0.5 and 2 units of alkaline phosphatase (200 units/ml) in TEAB, pH 8, were added to 90μL of 5 mM solution of FATP in microtubes and incubated for 40 min at 25°C. Samples were frozen and kept at −20°C before HPLC analysis. The analysis of FATP was performed by ion pair HPLC as described above. The full hydrolysis of FATP in phosphatase protection assay was usually achieved using 5 units of alkaline phosphatase (1 h, 25°C).

2.9. Formulation of Nanogel/FATP complexes

Nanogels can spontaneously form complexes with nucleoside 5'-triphosphates in aqueous media. In the first approach, Nanogel solution titrated with hydrochloric acid to pH 7.4 was mixed with the sodium salt of FATP at N/P ratio 3.5 and complex was allowed to form during

30 min. Then, an excess of non-bound FATP was removed by short dialysis (3 h, 4°C) in the membrane tube with a MW cutoff of 2,000 and the obtained Formulation *A* was freeze-dried. The drug content in this Formulation *A* was measured spectrophometrically and was usually equal to 14–17% by weight (low drug loading).

According to the second approach, Nanogel was initially converted to free ammonium salt by dialysis in SpectraPor membrane bags with a MW cutoff of 25,000 against 0.01% aqueous ammonia overnight. The solution was concentrated *in vacuo*, filtered and redissolved in water. Sodium salt of FATP was dissolved in water and passed through a short column with Dowex 50 x 6 in H^+ form to convert phosphates into free acid form. The column was then washed by water (2 x 15 ml), and the eluate was used directly for complex formation. Nanogel solution was titrated by triphosphate solution until pH reached 7.4. The final dispersion of the Nanogel/FATP complex (Formulation *B*) was freeze-dried. Formulation B obtained at these conditions has contained up to 30% of the bound FATP (high drug loading).

The dynamic light scattering measurements were performed using 'ZetaPlus' Zeta Potential Analyzer (Brookhaven Instruments, Santa Barbara, CA) equipped with 15 mV solid state laser operated at a laser wavelength of 635 nm and having the Multi-Angle Option at the angle of 90°. Effective hydrodynamic diameters of free and the FATP-loaded Nanogel particles were obtained at 25°C in phosphate buffer, pH 7.4, at concentration 0.1%.

2.10. Transmission electron microscopy (TEM)

Complexes of Nanogel (0.1% solution) with 1 mM $Cu(NO_3)_2$ were prepared in 10 mM tris-HCl, pH 7.4, and 0.1M NaCl at molar Cu/PEI ratio 10, which is equivalent to 10% of cupper (II) binding at saturation. Then, 100 mM ATP solution was added to obtain Nanogel/ATP complexes with N/P ratio 3. Following a short dialysis of the complexes in SpectraPor membrane tube with a MW cutoff of 2,000 against water, samples have been freeze-dried. Nanogel and drug-Nanogel dispersions for TEM were prepared at polymer concentration 0.01%.

2.11. In vitro drug release

Nanogel/FATP formulations obtained by two different ways as shown above and designated as Formulations *A* (low drug loading) and *B* (high drug loading) were dissolved in PBS to obtain 10 ml of 0.05% dispersion and the initial UV absorbance was measured at 260 nm using Perkin-Elmer spectrophotometer. These dispersions were placed in SpectraPor membrane bags with cutoff 2KDa, and dialyzed against PBS in a large 4L-beaker at 25°C. The withdrawn samples (3 ml) were analyzed spectrophotometrically at 260 nm for fludarabine and placed back into the dialysis bags. The obtained results have been plotted as % of FATP released from Nanogel carrier *vs.* time of incubation.

2.12. Cell cultures

Human breast carcinoma MCF-7 and colon carcinoma Caco-2 cells were obtained from the ACCC (Rockville, MD) and maintained in Dulbecco's minimal essential medium (DMEM) supplemented with nonessential amino acids, 2 mM of L-glutamine, 10% fetal bovine serum (FBS), penicillin (100 U/ml) and streptomycin (100 U/ml). All culture media were obtained from Gibco (Fisher Scientific, Pittsburgh, PA). MCF-7 cells were seeded at a density of 10,000 cells/well on 96-well plates, or 50,000 cells/well on 24-well plates and allowed to grow overnight for reattachment. Caco-2 cells were seeded at a density of 250,000 cells/insert on 6-wells Costar Transwell membrane inserts (polycarbonate filter, diameter of 24 mm and pore size of 0.4 mm) and used for permeation studies after reaching confluency (2–3 weeks).

2.13. Cytotoxicity analysis

Cytotoxicity of free and NATP-loaded Nanogel was assessed by a standard thiazolyl blue tetrazolium bromide (MTT) assay [29]. Briefly, serial dilutions of Nanogel or Nanogel/FATP complexes in assay buffer were incubated with the cells for 4 or 24 hours at 37°C. Samples were washed three times with 100 μl of assay buffer and grown for 3 days in a fresh culture medium changed daily. Then, 25 μl of MTT solution (5 mg/ml) was added and cells were incubated for 2 hours at 37°C in the dark. The medium and indicator dye were washed out by PBS and cells were lysed with 20% sodium dodecylsulfate in 50% aqueous dimethylformamide (100 μl) overnight at 37°C. Absorption was measured at 550 nm in Microplate reader and obtained values were expressed as a percentage of the values obtained for control cells to which no carriers were added. All measurements were repeated eight times. The IC_{50} values were calculated using the Prizm software (GraphPad).

2.14. Cellular accumulation

Cellular accumulation of Rh-labeled Nanogel was examined in MCF-7 cell monolayers as described earlier [30]. Attached overnight cells were washed and preincubated for 30 min with the serum-free assay buffer (122 mM NaCl, 25 mM $NaHCO_3$, 3 mM KCl, 1.2 mM Mg $(SO_4)_2$, 1.4 mM $CaCl_2$, 0.4 mM K_2HPO_4, 10 mM glucose and 10 mM HEPES). Then, cells were treated with 0.5 m1 of Nanogel or Nanogel/FATP complexes for 1-2 h at 37°C. After treatment, cells were washed three times with ice-cold PBS containing 1% BSA, and then solubilized in 1% Triton X-100 solution. Fluorescence associated with the cells was measured at λ_{ex}= 549 nm and λ_{em}= 577 nm and obtained values were normalized by protein content in each sample determined using Pierce BCA kit according to the manufacturer's protocol. All experiments were repeated in triplicate.

2.15. Permeation studies

Permeation studies were performed from apical to basolateral direction of confluent Caco-2 monolayers grown on polycarbonate membrane inserts as previously described [31]. Transepithelial electrical resistance (TEER) of the cell monolayers was controlled before starting the experiment. Only monolayers with a TEER value measured 30 min before the experiment higher than 450 omm/cm^2 were used. Cell monolayers were pre-incubated for 30 min with assay buffer added into both compartments of thermostated 6-well inserts maintained at 37°C. Following the incubation, the buffer in the apical compartment was replaced with Nanogel or Nanogel/FATP complexes containing a paracellular marker for cell monolayers, ^{3}H-labeled mannitol, and buffer in the basolateral compartment was replaced with fresh assay buffer. All experiments were conducted in triplicates. At different time points, solutions in the basolateral compartment were removed and analyzed for FATP by ion-pair HPLC. The apparent permeability coefficient (P_{app}) was calculated using the following equation:

$$P_{app} = (1 / AC_o) x\, dC / dt\,(cm / s)$$

where d*C*/d*t* is the steady-state rate of appearance of FATP at the basolateral side of the monolayers, C_o is the initial FATP concentration at the apical side, and *A* is the surface area of the membrane (4.71 cm^2) [22].

3. Results and discussion

3.1. Synthesis and properties of Nanogel carriers

Nanoscale hydrogel particles (Nanogels) have been synthesized by the "emulsification-solvent evaporation" method described previously [9]. Nanogel structure consists of 3D-network of

cross-linked polymer chains schematically presented in Figure 2. This network has a significant number of amino groups that are easily accessible for post-synthetic modification with fluorescent, radioactive or targeting ligands. Figure 2 illustrates the synthesis of folate-modified Nanogel for a specific cellular targeting via folate receptors. By this approach, the carbodiimide-activated folate forms with an equal probability both types of conjugate with Nanogels, via α-or γ-carboxyl group. Although, only one type of conjugate is active for targeting of folate receptors overexpressed in many cancer cells [24], the modification of Nanogel with multiple folate moieties (1 or 5% substitution of all amino groups in PEI) provides a sufficient quantity of the receptor-active conjugates. Composition and properties of synthesized Nanogels are presented in Table 1. The total nitrogen content and PEG/PEI molar ratio were calculated from elemental analysis data and proton NMR spectra measured in D_2O using integrals of CH_2O (δ 3.6, PEG) and $CH_2N/CH_2NH/CH_2NH_2$ (δ, 2.6–2.8, PEI) protons.

The ratio of polymer components in preparation of Nanogel carriers is an important parameter because it ascertains the gel rigidity and swelling capacity. Earlier, we have discovered that bulk hydrogels produced from bis-activated PEG (Mw 8,000) and PEI (Mw 25,000) at the weight ratio less than 2 (equal to the molar ratio 6) have demonstrated poor mechanical properties [9]. Rigidity and swelling capacity of hydrogels depend on polymer cross-linking degree. The latter may play also a decisive role in intracellular events following the cellular uptake of Nanogels. For example, a high efficacy of transfection with PEI-based DNA carriers is usually explained by endosomal disruption because of so-called “proton sponge” effect and swelling of PEI-based carriers in acidic environment [32]. Similarly, a considerable increase of Nanogel volume may accelerate endosomes disruption and cytosolic drug release. Therefore, we studied here the swelling degree of bulk PEG-*cl*-PEI hydrogel samples in order to determine an optimal weight ratio of polymer components. A set of hydrogels with PEG/PEI weight ratio from 2 to 10 have been prepared and their swelling degree was measured at different pH. The swelling degree increased as pH decreased. For example, at pH 4 the hydrogels volume grew more than twice compared to the volumes at pH 7. Practically all amino groups in the PEI backbone become protonated in acid conditions as it is evident from the curve of potentiometric titration of Nanogel (Figure 3A). This pH also exists in late endosomes, therefore, active protonation and swelling of Nanogels following endocytosis may facilitate the release of particles from endosomes in cytosol. For that reason, a PEG/PEI weight ratio from 3 to 4 (or molar ratios 9–12) may be considered as optimal for preparation of mechanically strong Nanogels with high swelling capacity. These studies demonstrated a low change in volume of hydrogels at PEG/PEI ratio >5 (Figure 3B). Hydrogels at pH 10 had the lowest volume. Evidently, the Nanogel structure is compacted at this pH, because no repulsion exists between uncharged polymer chains.

PEI is known to be a chelator of many metals that form strong coordination complexes with amino groups. The PEI content in Nanogel samples was determined by a quantitative colorimetric protocol using Cu(II) nitrate [26]. At the excess of Cu(II) reagent, blue complex with Nanogel contains 6 amino groups of PEI coordinated to one metal ion. Linear calibration curve was obtained in the range of polymer concentration of 50–500 μg/ml, and the calculated PEI amount in Nanogel samples was in good correlation with results of elemental analysis. Electron-contrasted Nanogel-Cu(II) complexes can be obtained at 10% of maximal metal saturation ratio and used for structural TEM studies of unloaded and drug-loaded Nanogels (Figure 4). The TEM pictures have demonstrated a macroporous structure of unloaded Nanogels and significant compaction of initially well-distributed PEI chains after the ATP binding. At used conditions, no neutral polymers (PEG) can be seen by electron microscopy.

3.2. Preparation of fludarabine 5'- triphosphate (FATP) and its formulation with Nanogel

FATP was synthesized starting from fludarabine 5'-monophosphate (FAMP) according to the method [27]. Using this simple procedure, FAMP was initially activated by 1,1'-carbonyldiimidazole and then, without isolation, was reacted with the excess of inorganic pyrophosphate in the form of tetra-n-butylammonium salt. The product, FATP, was purified from reagents by anion-exchange chromatography on Sephadex A-50 column and isolated with a yield of 65%. A modified analytical ion-pair HPLC protocol was developed to analyze purity of FATP and mixture of fludarabine and corresponding nucleoside 5'-phosphates obtained in the result of enzymatic hydrolysis *in vitro* [28]. We have used alkaline phosphatase in order to evaluate *in vitro* protection of nucleoside 5'-triphosphates in Nanogel formulations. Figure 5A illustrates HPLC profiles of a commercial ATP sample (line *a*) and products of its partial digestion by alkaline phosphatase (line *b*). At these conditions, each additional phosphate group in nucleoside 5'-phosphates has resulted in the increase of elution time by ca. 3 min. Analysis of the synthesized FATP and its partial enzymatic hydrolysate has demonstrated the same retention times (Figure 5B). Purity of the isolated FATP was usually >90%. The FATP in the form of complex with Nanogel was generally protected from an *in vitro* enzymatic degradation, as shown in Figure 5C. The results have demonstrated that only 10% of the Nanogel-encapsulated FATP was degraded following 1 h-incubation with alkaline phosphatase, whereas 70% of FATP in solution was found in dephosphorylated form at these conditions.

Two different approaches have been used for preparation of the Nanogel/FATP formulations. In the first method solutions of both Nanogel and FATP in salt forms were mixed at pH 7.4 to obtain both nitrogen (Nanogel) and phosphate (FATP) concentrations in the mixture at the N/P ratio equal to ~3.5, when complete neutralization of charges occurs in the complex [9]. At pH 7.4 approximately 50% of total amount of amino groups in Nanogel are protonated and capable to bind oppositely charged phosphate groups of FATP. This drug-Nanogel complex was rapidly dialyzed against water and lyophilized (*Formulation A*). In the second method, PEI-backbone of Nanogel was initially converted into a free amino form (having pH 10 in aqueous solution). FATP was converted from sodium salt into a free acid form (having pH 3.5 in aqueous solution) and immediately used for complexion with Nanogel. Solution of Nanogel was titrated by the solution of FATP up to pH 7.4, and the formed complex was lyophilized (*Formulation B*). The obtained drug loading in the *Formulation A* prepared at pH 7.4 was twice as low compared to the *Formulation B* prepared at pH 3.5 as evident from acid titration properties of branched PEI (Figure 3A). *In vitro* drug release from both Nanogel formulations has showed a very similar kinetics, however, in terms of absolute amount of passively released FATP the *Formulation B* was better (33% after 24 h-incubation) than the *Formulation A* (68%), as shown in Figure 6. Therefore, our final choice was made in favor of the *Formulation B*, and all results reported in this paper are related to this type of Nanogel/FATP polyplex. HPLC analysis has proved that the drug-Nanogel formulation can be stored in lyophilized form at 4°C for many months without degradation of the encapsulated FATP. Particle size after the restitution of lyophilized drug-Nanogel formulation in PBS was practically the same as in the freshly prepared polyplex (data not shown). It is very well soluble in water, and the FATP content can be easily analyzed by UV absorbance at 260 nm.

3.3. Cytotoxicity studies

Cytotoxicity of phosphorylated drug (FATP), Nanogel and FATP/Nanogel complex was evaluated in MCF-7 cell culture using a MTT cell viability assay [29]. In order to detect how the Nanogel encapsulation affects the cytotoxic properties of FATP, concentration of drug-Nanogel formulations should be in the range of negligible cytotoxicity. Firstly, we have compared cytotoxicity of Nanogel carriers with a various PEG/PEI molar ratios. At fixed 0.01% concentration and 4h-incubation time, Nanogel cytotoxicity in MCF-7 cells was found to inversely depend on PEG/PEI molar ratio, showing low cytotoxicity at the ratio 9 or higher

(Figure 7A). Therefore, Nanogel carriers used in biological studies have been synthesized at molar ratio 12. At 4h-incubation time these Nanogels have demonstrated a moderate cytotoxicity level with IC_{50} = 0.7 mg/ml (0.07%). Longer incubation periods would not adequately reflect the cytotoxic effect of encapsulated nucleoside 5'-triphosphates, which will likely be completely degraded (dephosphorylated) during a prolonged cell treatment. Therefore, we used a relatively short 4h-incubation period that is sufficient for internalization of drug-Nanogel formulations for comparing cytotoxicities of FATP and FATP-loaded Nanogel. The cell survival following the 4h-treatment with 0.01% solution of unloaded Nanogel was higher than 90%. When 0.01% dispersion of Nanogel/FATP polyplex was applied, it was equivalent to application of 50 μM FATP. At used experimental conditions, the Nanogel/FATP complex was cytotoxic at significantly lower concentrations (IC_{50} = 3 μM) than for FATP alone (IC_{50} = 27 μM) or non-phosphorylated nucleoside analog, fludarabine (IC_{50} = 30 μM) (Figure 7B). This result clearly demonstrates that Nanogel-encapsulated phosphorylated nucleoside analogs are significantly more cytotoxic to proliferating cancer cells than initial drugs themselves, and this effect is not due to an additional cytotoxicity of Nanogel carriers. Evidently, the slow passive drug release from Nanogels into cytosol also cannot explain the observed phenomenon. An interesting feature of cationic Nanogels as drug carriers is their ability to trigger drug release in the result of interaction with anionic (hydrophobic) compounds competing for the same drug binding sites in Nanogels. It seems that interactions of Nanogel particles with cellular membrane and its components comprise an important part of intracellular drug release from Nanogel complexes. This mechanism, initially proposed in the review [12], was recently studied in our laboratory and obtained results will be published elsewhere.

3.4. Drug transport in vectorized Nanogel-FATP formulations

Initially, the cellular association of non-vectorized and folate-modified Nanogels carrying a rhodamine label was evaluated in human breast carcinoma MCF-7 cells. These cancer cells are expressing a certain level of folate receptors and have been previously studied with folate-vectorized polymer-drug formulations [33,34]. Cellular association of non-vectorized Nanogel was slightly increased after 2h-incubation with cell monolayers, which is indicative of the rapid saturation of Nanogel binding sites on the cellular surface (Figure 8). At the same time, folate-modified Nanogels have showed marked increase of cellular association, evidently, because of the effective process of receptor-mediated endocytosis and recycling of folate receptors after internalization of Nanogel particles. Overall, a significant 8-fold increase in cellular uptake was found for the folate-modified Nanogel (5% folate substitution of amino groups) compared to a non-vectorized Nanogel following 2h-incubation with MCF-7 cells.

In the next experiment, a transcellular transport of FATP and FATP-loaded Nanogel carriers was examined using an *in vitro* model of intestinal barrier, Caco-2 cell monolayers. Requirement for efficient intestinal uptake of folate determines the high density of folate receptors in Caco-2 cells [35]. Folate transporter has been found also in the normal human colonic apical membranes [36]. The concentration of FATP transported to the basolateral compartment was expressed as percentage of initial concentration of FATP in the apical compartment. The transfer of Nanogels was evidently performed via transcytosis route because no change in paracellular transport of mannitol has been noticed during the experiment (data not shown). The transcytosis of FATP in the form of folate-Nanogel-formulations has been up to 4 times more efficient than that of FATP alone. Moreover, non-formulated FATP was found in the basolateral compartment mostly in dephosphorylated form after the transcytosis, while Nanogel formulations have maintained integrity up to 85% of the initial FATP (data not shown). Drug transfer (%) from apical to basolateral side of Caco-2 monolayers and calculated permeability coefficients are shown in Table 2. Only a moderate transfer increase observed for vectorized Nanogel with folate substitution of 1% of amino groups was evidently a result of

insufficient ligand density on the surface of Nanogel carrier. The increase in the ligand density from 1 to 5% has resulted in a 2-fold elevation of the drug transfer rate. Taken together, these results clearly demonstrate an increased ability of Nanogels after modification with folate to bind cancer cells expressing folate receptors and efficiently carry the encapsulated drug across cellular monolayers in the model of gastrointestinal tract. Certainly, systematic studies need to be performed to evaluate application of vectorized Nanogels for cancer drug delivery that can significantly increase the local effect of cytotoxic nucleoside analogs, reduce unwanted biodistribution and complications related to their systemic toxicity. Recently, vectorized Nanogels have been shown to enhance transport of oligonucleotides across the blood-brain barrier following an intravenous administration [25]. Additionally, the efficient transport and protection of phosphorylated drugs against digestion in gastrointestinal tract can add a new dimension to the application of Nanogel as drug carriers.

4. Conclusions

The major problem of cancer chemotherapy by cytotoxic nucleoside analogs is a tissue-selective and often low-effective activation of these prodrugs after *per oral* or systemic administration, which requests for increased therapeutic doses and causes various systemic toxic effects in cancer patients. Development of drug delivery systems could provide solution to many of these concerns. We have demonstrated that Nanogel drug carriers in many aspects could be considered as promising candidates for encapsulation and delivery of phosphorylated nucleoside analogs. First, delivery of these drugs in active form, such as nucleoside analog 5'-triphosphates, could significantly increase therapeutic efficacy and immediate effect on actively proliferating cancer cells. Second, Nanogel formulations could significantly extend choice of usable cytotoxic drugs because there will be no need for the drug activation *in vivo*. Many drugs previously found as inactive to specific types of cancer could become very efficient in phosphorylated form [36], and, therefore, could be tested again in the form of drug-Nanogel formulations. Third, the administered dose of Nanogel-encapsulated phosphorylated drugs could be significantly lower compared to the dose of corresponding nucleoside analogs.

Several unique properties of Nanogel such as (i) low buoyant density, (ii) excellent solubility, (iii) large pore size important for easy drug loading using ion exchange properties of the network, (iv) polymer envelope surrounding the carrier and protecting encapsulated biodegradable drugs, and (v) efficient storage of drug-Nanogel formulations in lyophilized form could make Nanogel a "carrier-of-choice" for many anionic low molecular weight drugs, including the nucleoside analog 5'-triphosphates. Synthesized Nanogels have showed low cytotoxicity as carriers; however, they have markedly enhanced cytotoxic action of the encapsulated drugs. These formulation could be a novel promising drug form that exhibit an efficient therapeutic activity but without elevated systemic toxicity.

Supplementary Material

Refer to Web version on PubMed Central for supplementary material.

Acknowledgements

The present work was supported by National Cancer Institute grant R01 CA102791. Supratek Pharma Inc. (Canada) is acknowledged for financial support of initial phase of this investigation. The authors would like to thank Tom Bargar for assistance in TEM, and Shu Li for valuable help in cell culture work.

References

1. Duncan R. The dawning era of polymer therapeutics. Nat Rev Drug Discov 2003;2:347–360. [PubMed: 12750738]

2. Zhang S, Xu Y, Wang B, Qiao W, Liu D, Li Z. Cationic compounds used in lipoplexes and polyplexes for gene delivery. J Control Release 2004;100:165–180. [PubMed: 15544865]

3. Boussif O, Lezoualc'h F, Zanta MA, Mergny MD, Scherman D, Demeneix B, Behr JP. A versatile vector for gene and oligonucleotide transfer into cells in culture and in vivo: polyethylenimine. Proc Natl Acad Sci U S A 1995;92:7297–7301. [PubMed: 7638184]

4. De Smedt SC, Demeester J, Hennink WE. Cationic polymer based gene delivery systems. Pharm Res 2000;17:113–126. [PubMed: 10751024]

5. Kircheis R, Wightman L, Wagner E. Design and gene delivery activity of modified polyethylenimines. Adv Drug Deliv Rev 2001;53:341–358. [PubMed: 11744176]

6. Lemkine GF, Demeneix BA. Polyethylenimines for in vivo gene delivery. Curr Opin Mol Ther 2001;3:178–182. [PubMed: 11338931]

7. Kwok KY, Yang Y, Rice KG. Evolution of cross-linked non-viral gene delivery systems. Curr Opin Mol Ther 2001;3:142–146. [PubMed: 11338926]

8. Ogris M, Wagner E. Tumor-targeted gene transfer with DNA polyplexes. Somat Cell Mol Genet 2002;27:85–95. [PubMed: 12774943]

9. Vinogradov SB, Kabanov EA. Poly(ethylene glycol)-polyethylenimine NanoGel particles: novel drug delivery systems for antisense oligonucleotides. Colloids and Surfaces B: Biointerfaces 1999;16:291–304.

10. Lemieux P, Vinogradov SV, Gebhart CL, Guerin N, Paradis G, Nguyen HK, Ochietti B, Suzdaltseva YG, Bartakova EV, Bronich TK, St-Pierre Y, Alakhov VY, Kabanov AV. Block and graft copolymers and NanoGel copolymer networks for DNA delivery into cell. J Drug Target 2000;8:91–105. [PubMed: 10852341]

11. TKV, Bronich; Kabanov, AVSV. Interaction of nanosized copolymer networks with oppositely charged amphiphilic molecules. NanoLetters 2000;1:535–540.

12. Vinogradov SV, Bronich TK, Kabanov AV. Nanosized cationic hydrogels for drug delivery: preparation, properties and interactions with cells. Adv Drug Deliv Rev 2002;54:135–147. [PubMed: 11755709]

13. Galmarini CM, Mackey JR, Dumontet C. Nucleoside analogues and nucleobases in cancer treatment. Lancet Oncol 2002;3:415–424. [PubMed: 12142171]

14. Robak T. Purine nucleoside analogues in the treatment of myleoid leukemias. Leuk Lymphoma 2003;44:391–409. [PubMed: 12688309]

15. Van Rompay AR, Johansson M, Karlsson A. Substrate specificity and phosphorylation of antiviral and anticancer nucleoside analogues by human deoxyribonucleoside kinases and ribonucleoside kinases. Pharmacol Ther 2003;100:119–139. [PubMed: 14609716]

16. Huang P, Plunkett W. Fludarabine- and gemcitabine-induced apoptosis: incorporation of analogs into DNA is a critical event. Cancer Chemother Pharmacol 1995;36:181–188. [PubMed: 7781136]

17. Gandhi V, Plunkett W. Cellular and clinical pharmacology of fludarabine. Clin Pharmacokinet 2002;41:93–103. [PubMed: 11888330]

18. Adachi M, Reid G, Schuetz JD. Therapeutic and biological importance of getting nucleotides out of cells: a case for the ABC transporters, MRP4 and 5. Adv Drug Deliv Rev 2002;54:1333–1342. [PubMed: 12406648]

19. Damaraju VL, Damaraju S, Young JD, Baldwin SA, Mackey J, Sawyer MB, Cass CE. Nucleoside anticancer drugs: the role of nucleoside transporters in resistance to cancer chemotherapy. Oncogene 2003;22:7524–7536. [PubMed: 14576856]

20. Oussoren C, Magnani M, Fraternale A, Casabianca A, Chiarantini L, Ingebrigsten R, Underberg WJ, Storm G. Liposomes as carriers of the antiretroviral agent dideoxycytidine-5′-triphosphate. Int J Pharm 1999;180:261–270. [PubMed: 10370196]

21. Di Paolo A. Liposomal anticancer therapy: pharmacokinetic and clinical aspects. J Chemother 2004;16(Suppl 4):90–93. [PubMed: 15688620]

22. Artursson P, Palm K, Luthman K. Caco-2 monolayers in experimental and theoretical predictions of drug transport. Adv Drug Deliv Rev 2001;46:27–43. [PubMed: 11259831]

23. Watts PJ, Davies MC, Melia CD. Microencapsulation using emulsification/solvent evaporation: an overview of techniques and applications. Crit Rev Ther Drug Carrier Syst 1990;7:235–259. [PubMed: 2073688]

24. Leamon CP, DePrince RB, Hendren RW. Folate-mediated drug delivery: effect of alternative conjugation chemistry. J Drug Target 1999;7:157–169. [PubMed: 10680972]
25. Vinogradov SV, Batrakova EV, Kabanov AV. Nanogels for oligonucleotide delivery to the brain. Bioconjug Chem 2004;15:50–60. [PubMed: 14733583]
26. Ungaro F, De Rosa G, Miro A, Quaglia F. Spectrophotometric determination of polyethylenimine in the presence of an oligonucleotide for the characterization of controlled release formulations. J Pharm Biomed Anal 2003;31:143–149. [PubMed: 12560058]
27. Hoard DE, Ott DG. Conversion Of Mono- And Oligodeoxyribonucleotides To 5-Triphosphates. J Am Chem Soc 1965;87:1785–1788. [PubMed: 14289336]
28. Decosterd LA, Cottin E, Chen X, Lejeune F, Mirimanoff RO, Biollaz J, Coucke PA. Simultaneous determination of deoxyribonucleoside in the presence of ribonucleoside triphosphates in human carcinoma cells by high-performance liquid chromatography. Anal Biochem 1999;270:59–68. [PubMed: 10328765]
29. Mosmann T. Rapid colorimetric assay for cellular growth and survival: application to proliferation and cytotoxicity assays. J Immunol Methods 1983;65:55–63. [PubMed: 6606682]
30. Vinogradov S, Batrakova E, Li S, Kabanov A. Polyion complex micelles with protein-modified corona for receptor-mediated delivery of oligonucleotides into cells. Bioconjug Chem 1999;10:851–860. [PubMed: 10502353]
31. Hidalgo IJ, Raub TJ, Borchardt RT. Characterization of the human colon carcinoma cell line (Caco-2) as a model system for intestinal epithelial permeability. Gastroenterology 1989;96:736–749. [PubMed: 2914637]
32. Zuber G, Dauty E, Nothisen M, Belguise P, Behr JP. Towards synthetic viruses. Adv Drug Deliv Rev 2001;52:245–253. [PubMed: 11718949]
33. Lee ES, Na K, Bae YH. Polymeric micelle for tumor pH and folate-mediated targeting. J Control Release 2003;91:103–113. [PubMed: 12932642]
34. Lee ES, Na K, Bae YH. Doxorubicin loaded pH-sensitive polymeric micelles for reversal of resistant MCF-7 tumor. J Control Release 2005;103:405–418. [PubMed: 15763623]
35. Doucette MM, Stevens VL. Folate receptor function is regulated in response to different cellular growth rates in cultured mammalian cells. J Nutr 2001;131:2819–2825. [PubMed: 11694602]
36. Dudeja PK, Kode A, Alnounou M, Tyagi S, Torania S, Subramanian VS, Said HM. Mechanism of folate transport across the human colonic basolateral membrane. Am J Physiol Gastrointest Liver Physiol 2001;281:G54–60. [PubMed: 11408255]
37. McGuigan C, Kinchington D, Wang MF, Nicholls SR, Nickson C, Galpin S, Jeffries DJ, O'Connor TJ. Nucleoside analogues previously found to be inactive against HIV may be activated by simple chemical phosphorylation. FEBS Lett 1993;322:249–252. [PubMed: 8387430]

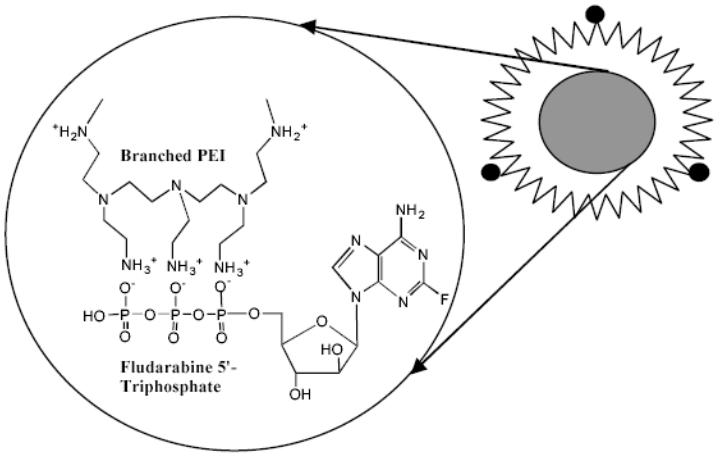

Figure 1.
Vinogradov et al. Polyplex Nanogel…

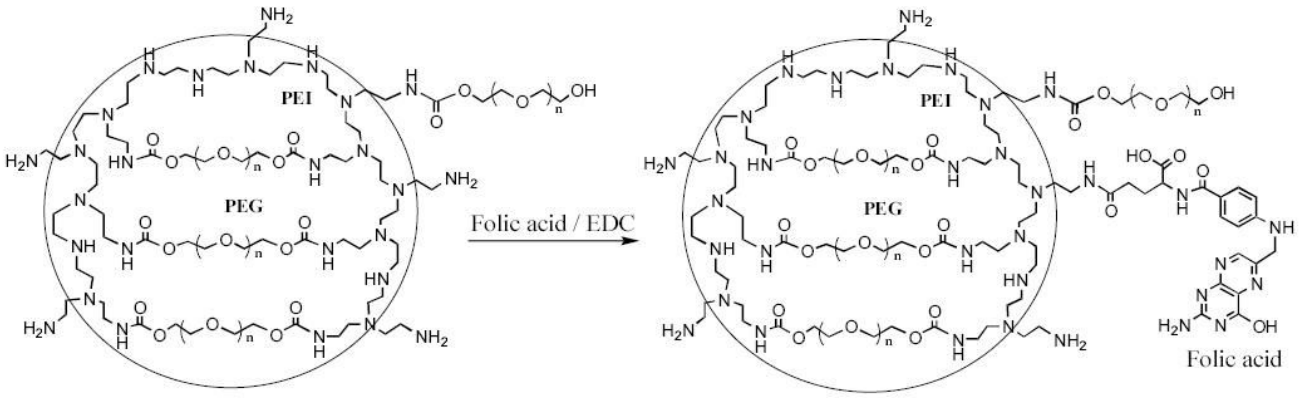

Figure 2.
Vinogradov et al. Polyplex Nanogel…

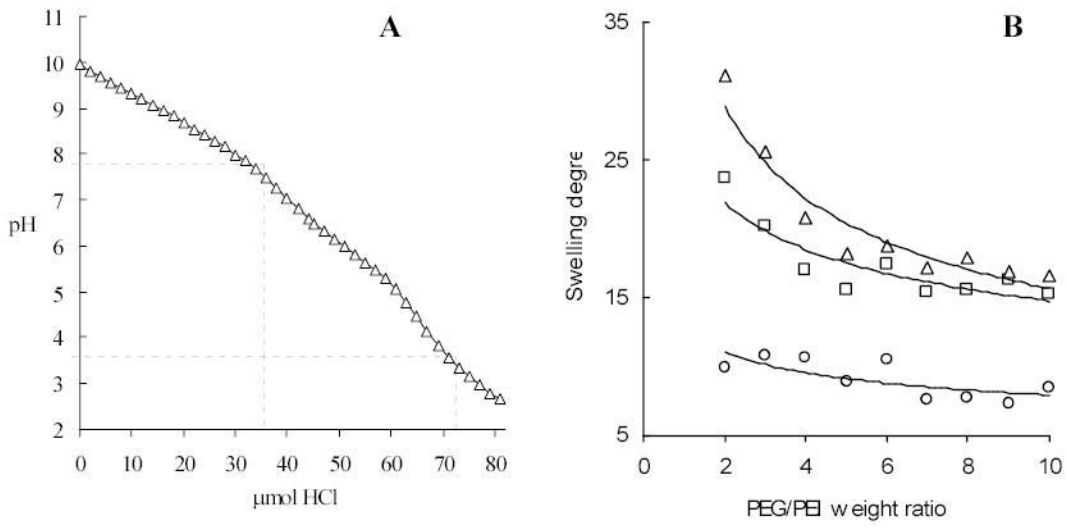

Figure 3.
Vinogradov et al. Polyplex Nanogel…

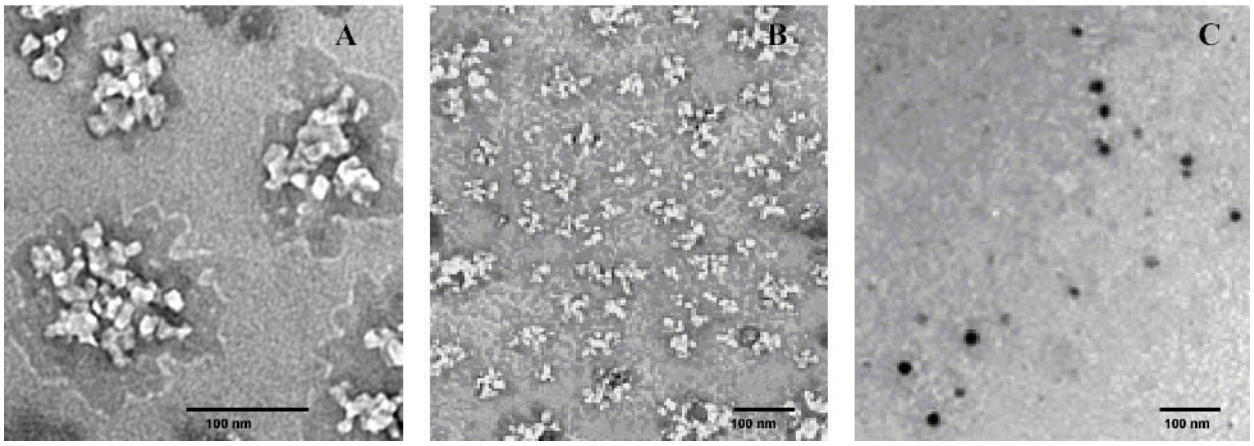

Figure 4.
Vinogradov et al. Polyplex Nanogel…

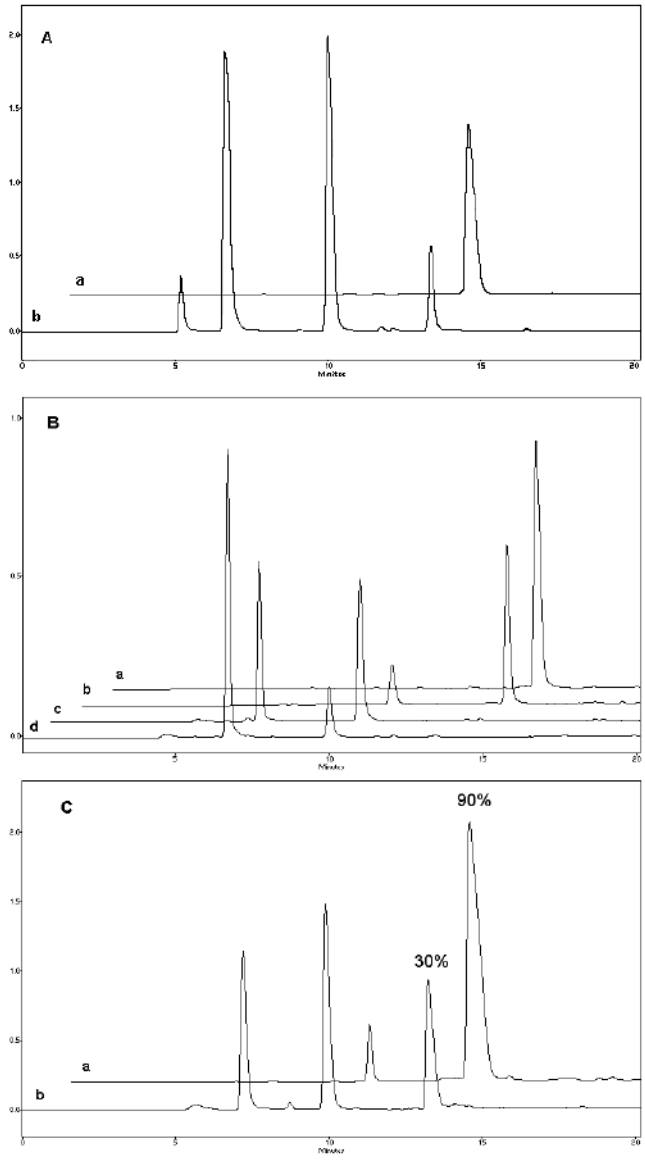

Figure 5.
Vinogradov et al. Polyplex Nanogel…

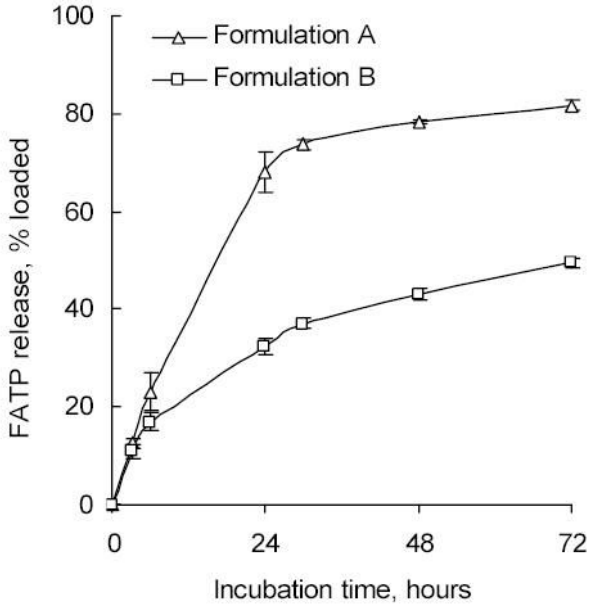

Figure 6.
Vinogradov et al. Polyplex Nanogel…

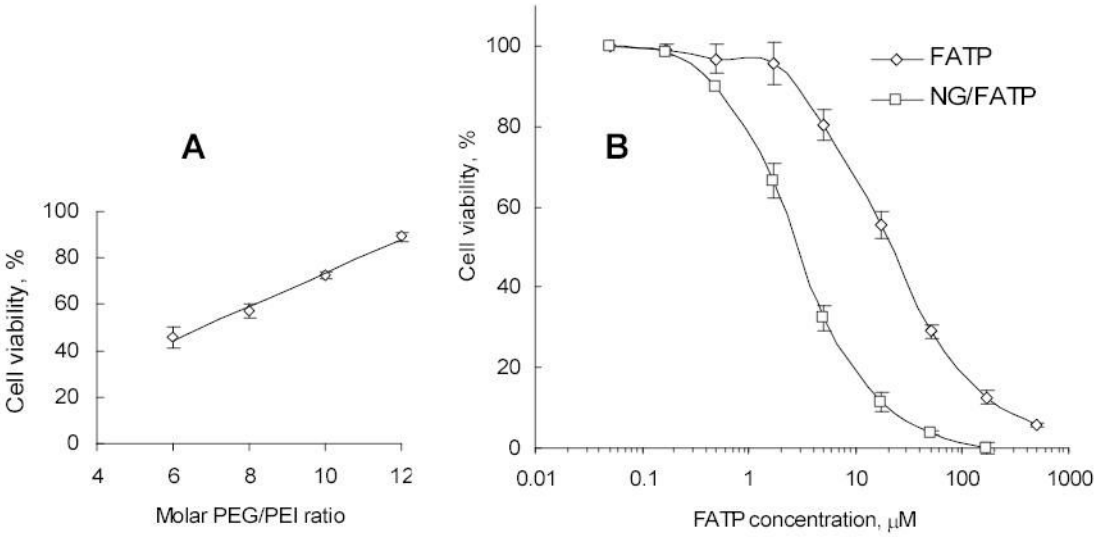

Figure 7.
Vinogradov et al. Polyplex Nanogel…

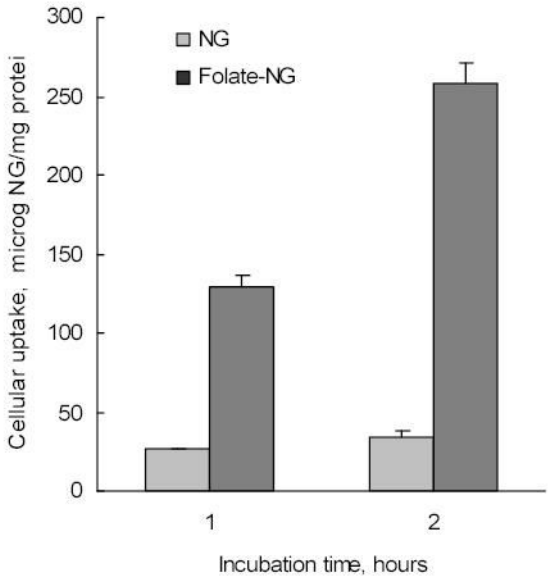

Figure 8.
Cellular accumulation of both rhodamine-labeled Nanogels and folate-Nanogels in human breast carcinoma MCF-7 cell monolayers.

Table 1

Analytical and hydrodynamic properties of Nanogel carriers and Nanogel/FATP complexes

Nanogels	Reactive PEG/ PEI molar ratio	Folate %	Nitrogen content, % (μmol/mg Nanogel)[a]	FATP loading, μg/mg Nanogel[b]	Hydrodynamic diameter, nm, (FATP-loaded Nanogel)[c]
NG6	6	-	12.9 (9.2)	300	373±25 (150±9)
NG8	8	-	8.8 (6.3)	230	152±6 (65±5)
NG10	10	-	7.7 (5.5)	200	114±4 (43±1)
NG12	12	-	6.6 (4.7)	150	70±6 (30±1)
Folate(1%)NG	12	1	6.7 (4.8)	150	65±4 (26±2)
Folate(5%)NG	12	5	7.0 (5.0)	130	58±5 (28±3)

[a] The total nitrogen content values (%) obtained by elemental analysis and converted into μmol/mg of Nanogel using coefficient 14 μg/μmol of nitrogen.

[b] The FATP loading was calculated based on titration data for 1% Nanogel (free amine form) and 1% FATP solutions (free acid form) up to pH7.

[c] The hydrodynamic diameter was measured for 0.1% Nanogel or Nanogel/FATP solutions in PBS. The results are average values of three measurements ± SEM.

Table 2

Drug transfer through Caco-2 cell monolayers *in vitro* and the apparent permeability (P_{app}) coefficient for FATP and Nanogel/FATP complexes

Drug formulation[a]	FATP transfer, %[b]	P_{app}, cm/s x 10^6
FATP	12	6.47
Nanogel/FATP	15.6	6.95
Folate (1%)-Nanogel/FATP	23.3	11.7
Folate (5%)-Nanogel/FATP	45.8	25.46

[a] Based of spectrophotometric analysis, folate-Nanogels contained ca. 1 or 5% of the total amino groups substituted.

[b] Data obtained after 60 min-incubation with FATP (0.2 mg/ml) or complexes.